Molecular Biology of the Cell
Vol. 19, 5032–5046, December 2008

Rap1 Activation in Collagen Phagocytosis Is Dependent on Nonmuscle Myosin II-A

Pamela D. Arora,* Mary Anne Conti,† Shoshana Ravid,‡ David B. Sacks,§ Andras Kapus,‖ Robert S. Adelstein,† Anne R. Bresnick,¶ and *Christopher A. McCulloch*

*CIHR Group in Matrix Dynamics, University of Toronto, Toronto, ON M5S 3E2, Canada; †Laboratory of Molecular Cardiology, National Heart, Lung, and Blood Institute, National Institutes of Health, Bethesda, MD 20892; ‡Hadassah Medical School, The Hebrew University, Jerusalem 91120, Israel; §Harvard Medical School, Brigham and Women's Hospital, Boston, MA 02115; ‖St. Michael's Hospital Research Institute, Toronto, ON, M5B 1W8, Canada; and ¶Albert Einstein College of Medicine, Bronx, NY 10461

Submitted April 25, 2008; Revised August 26, 2008; Accepted September 9, 2008
Monitoring Editor: Erika Holzbaur

Rap1 enhances integrin-mediated adhesion but the link between Rap1 activation and integrin function in collagen phagocytosis is not defined. Mass spectrometry of Rap1 immunoprecipitates showed that the association of Rap1 with nonmuscle myosin heavy-chain II-A (NMHC II-A) was enhanced by cell attachment to collagen beads. Rap1 colocalized with NM II-A at collagen bead-binding sites. There was a transient increase in myosin light-chain phosphorylation after collagen-bead binding that was dependent on myosin light-chain kinase but not Rho kinase. Inhibition of myosin light-chain phosphorylation, but not myosin II-A motor activity inhibited collagen-bead binding and Rap activation. In vitro binding assays demonstrated binding of Rap1A to filamentous myosin rods, and in situ staining of permeabilized cells showed that NM II-A filaments colocalized with F-actin at collagen bead sites. Knockdown of NM II-A did not affect talin, actin, or β1-integrin targeting to collagen beads but targeting of Rap1 and vinculin to collagen was inhibited. Conversely, knockdown of Rap1 did not affect localization of NM II-A to beads. We conclude that MLC phosphorylation in response to initial collagen-bead binding promotes NM II-A filament assembly; binding of Rap1 to myosin filaments enables Rap1-dependent integrin activation and enhanced collagen phagocytosis.

INTRODUCTION

Fibroblasts are the predominant cells of soft connective tissues and mediate collagen synthesis and collagen degradation to affect matrix remodeling, thereby preserving tissue homeostasis. Matrix remodeling is dependent on intracellular collagen degradation by phagocytosis, an important pathway for collagen turnover in tissues with rapid turnover rates (e.g., involuting uterus and periodontium; Everts *et al.*, 1996). Disruption of the intracellular collagen degradation pathway leads to imbalances in matrix homeostasis with clinical consequences including tissue overgrowth and fibrosis (McCulloch, 2004).

Phagocytosis is a receptor-driven process that is dependent on remodeling of the actin cytoskeleton and shares some of the cytoskeletal regulatory components involved in cell adhesion and migration. In response to extracellular signals including particle binding, small GTPases are activated to coordinate actin assembly and integrin activation during spreading and phagocytosis (Price *et al.*, 1998; Del Pozo *et al.*, 2002; Cougoule *et al.*, 2004). Studies of actin- and integrin-dependent collagen phagocytosis and its associated regulatory systems are facilitated by models that use loading of fibroblasts on collagen-coated latex beads (Grinnell, 1980; McAbee and Grinnell, 1983; Arora *et al.*, 2003). These models recapitulate some of the processes observed in spreading cells on tissue culture plates and show that integrin-mediated cell adhesion to the extracellular matrix is a critical step in collagen phagocytosis (Arora *et al.*, 2005).

The recruitment and function of Rho GTPases, specifically at sites of cell attachment to the extracellular matrix, are crucial for cell adhesion, spreading, and phagocytosis (Price *et al.*, 1998; Cougoule *et al.*, 2006; Hall *et al.*, 2006). The Rho family of small GTPases, which includes Rho, Rac, and Cdc42, are implicated in actomyosin-dependent processes and in actin reorganization processes crucial for phagocytosis. In macrophages responding to lipopolysaccharide, functional activation of $\alpha M\beta_2$-integrin facilitates phagocytosis of C3bi-opsonized targets and is controlled by the small GTPase Rap1 (Caron *et al.*, 2000). Rap1 has been implicated in the control of cell adhesion in a variety of cell types (Bos, 2005; Kinashi and Katagiri, 2005; Retta *et al.*, 2006). In *Dictyostelium discoideum*, Rap1 has been linked to cytoskeletal regulation, phagocytosis, and response to osmotic stress (Rebstein *et al.*, 1993; Kang *et al.*, 2002). Rap1 is thought to control cell adhesion by interacting with adaptor proteins that may regulate and control the cytoskeleton (Jeong *et al.*,

This article was published online ahead of print in *MBC in Press* (http://www.molbiolcell.org/cgi/doi/10.1091/mbc.E08–04–0430) on September 17, 2008.

Address correspondence to: Christopher A. McCulloch (mccculloch@utoronto.ca).

Abbreviations used: GST, glutathione-*S*-transferase; RBD, Ras-binding domain; MLC, myosin light chain; NM II-A, non-muscle myosin-II-A; NMHC II-A, non-muscle myosin II-A heavy chain; NMHC II-B, non-muscle myosin II-B heavy chain; MLCK, myosin light-chain kinase.

2007). Several Rap1 effectors (e.g., RIAM) induce lamellipodia formation and localize to sites of membrane protrusion (Lafuente *et al.*, 2004) and are critical for formation of integrin-associated complexes (Han *et al.*, 2006).

Integrins are heterodimeric adhesion molecules that bind extracellular matrix proteins and can activate a large group of signaling molecules, resulting in "outside-in" signaling (Mould and Humphries, 2004). Conversely, integrins are modified allosterically by intracellular signals that regulate integrin affinity, a process designated as "inside-out" signaling (Hughes and Pfaff, 1998). One of the consequences of outside-in signaling arising from integrin-mediated adhesion and cell spreading is the activation of Rho, Rac, and Cdc42. Although Rap1 activates β1-integrins (de Bruyn *et al.*, 2002; Bos, 2005), an example of inside-out signaling, it is established in human neutrophils that Rap1 and Rap2 are loaded with GTP after engagement of β2-integrins, indicating that β2-integrin outside-in signaling may contribute to Rap activation (Jenei *et al.*, 2006). Currently it is not understood how Rap localizes to particle binding sites and is activated in integrin-mediated phagocytosis.

A large superfamily of myosin molecules supports actin-related cellular functions (Pollard *et al.*, 1991; Cheney and Mooseker, 1992). Nonmuscle myosin II (NM II) is an actin-based motor protein that plays important roles in a wide variety of cellular processes (Sellers, 2000), including stress fiber organization (Chrzanowska-Wodnicka and Burridge, 1996). Currently, the regulation of NM II filament assembly in living cells is poorly defined, but recent studies have shown that phosphorylation of myosin light chain (MLC) at Thr18/Ser19 stabilizes NM II filaments in epithelial cells, suggesting that MLC phosphorylation is involved in regulation of NM II assembly (Watanabe *et al.*, 2007). Notably, one mechanism by which Rap1 controls cell adhesion in *D. discoideum* involves the regulation of NM II assembly (Jeon *et al.*, 2007). In macrophages, Rho activity and NM II are required for actin cup assembly during complement receptor but not FCγR-mediated phagocytosis. In contrast, with respect to particle internalization, NM II is required for both complement receptor and FCγR-mediated phagocytosis (Olazabal *et al.*, 2002). However, the roles of NM II in integrin activation and collagen phagocytosis are not defined.

Here we have identified NM II-A as a Rap1-interacting molecule in the binding step of collagen phagocytosis. We show that NM II-A filaments are required for Rap1 recruitment and activation, essential processes in β1-integrin–mediated collagen phagocytosis. Rap1 interaction with NM II-A restricts Rap1 to sites of collagen phagocytosis and functionally amplifies the integrin adhesion signal.

MATERIALS AND METHODS

Reagents

Latex (2-μm diameter) beads were purchased from Polysciences (Warrington, PA). Antibodies to β-actin (clone AC-15), GAPDH, vinculin, talin, bovine type 1 collagen (clone COL-1), fluorescein isothiocyanate (FITC)-conjugated goat anti-mouse (GAM) antibody, tetra-methyl rhodamine isothiocyanate (TRITC)-phalloidin, and myosin light-chain kinase (MLCK) antibody were from Sigma (St. Louis, MO). Rat monoclonal mouse β_1 integrin antibodies (clones KM16, 9EG7, and 18) were obtained from BD Biosciences PharMingen (San Jose, CA). The blocking antibody for α2β1 (clone BMA2.1) was from Chemicon (Temecula, CA). FITC-goat anti-rat antibody was purchased from Cedarlane Laboratories (Hornby, ON, Canada). Antibodies to Rap1 and total β1-integrin (clone N-20) were from Santa Cruz Biotechnology (Santa Cruz, CA). Immobilized protein G was obtained from Pierce (Rockford, IL). The antibody to NMHC II-A (BT-564) was from Biomedical Technologies (Stoughton, MA) and mAb to NMHC II-B (CMII23) was from the Developmental Studies Hybridoma Bank (University of Iowa, Iowa City, IA). MLC and phospho-MLC antibodies (P-Ser19) were purchased from Cell Signaling Technologies (Beverly, MA).

Plasmids

Green fluorescent protein (GFP)-tagged constructs of Rap1 were from M. Philips (New York University). To measure Ras activity of Rap1, binding of GDP-Ras and GTP-Ras was assayed using a glutathione *S*-transferase (GST) fusion of the Ras-binding domain (RBD; C-terminal 97 residues) from the downstream effector RalGDS. BL21 (DE3) LysE cells were transformed with pGEX-RBD plasmid (provided by L.A. Quilliam, Indiana University). The protein was expressed and isolated as described previously (Castro *et al.*, 2005). GST-bound RBD was stable for several weeks after preparation. GFP-NM II-A was purchased from Addgene (Cambridge, MA). GFP-NM II-A N93K was a gift from Alan F. Horwitz (University of Virginia, Charlottesville, VA). mCherry NM II-A was provided by T. Egelhoff (Case Western Reserve University, Cleveland, OH).

Cells

3T3 cells were cultured in DMEM supplemented with 10% fetal calf serum and 0.1% antibiotics. RW4, NMHC II-A null, and NMHC II-B null and wild-type (WT) embryonic stem cells were cultured as described previously (Conti *et al.*, 2004).

Collagen-Bead Binding and Bead Internalization

Collagen-coated latex beads were applied to microbiological dishes as described previously (Arora *et al.*, 2003). The number of beads plated per dish was adjusted to produce bead-to-cell ratios specific for each experiment, and these ratios were 4:1 for microscope or biochemical-based assays and were 6:1 for flow cytometry assays. We have not found differences in the rates of binding or internalization for these different bead ratios. For evaluation of collagen bead internalization, FITC-collagen–coated beads were incubated with cells for timed incubation periods. Internalization was stopped by cooling on ice. Fluorescence from extracellular beads was quenched by trypan blue; internalized beads retained their bead-associated fluorescence (Arora *et al.*, 2000). Uptake of fluorescence collagen films was conducted as described previously (Lee *et al.*, 2006). In experiments to assess the impact of collagen rigidity on internalization, cells were plated on either stiff collagen or soft collagen as described (Arora *et al.*, 1999). These collagen films were labeled with FITC, and cells were incubated overnight, trypsinized, and analyzed for internalized collagen by flow cytometry.

Isolation of Bead-attached Proteins and Immunoprecipitation

Cell suspensions were allowed to attach to bead-coated dishes for 20 min. Floating cells were aspirated and replaced with media warmed to 37°C to synchronize phagocytosis. Cells and collagen-coated latex beads were collected with a cell scraper into buffer (10 mM Tris, 1 mM NaF, 10 mM iodoacetamide, pH 7.5) containing protease inhibitors (Sigma) and incubated on ice for 20 min before cells were passed through 25-gauge needle (five times). Lysates were centrifuged and fractionated into cytosolic (supernatant) and pellet fractions (membrane). Pellets were solubilized in extraction buffer (1% Triton X-100, 150 mM NaCl, 10 mM Tris-HCl, pH 7.2, 1 mM Na_3VO_4, 20 μg/ml aprotinin, 1 μg/ml Pefabloc). Equal amounts of proteins were incubated with antibodies to Rap1 and β1-integrin to form immunocomplexes that were captured on Sepharose-G beads (Pierce). Samples were boiled, separated on SDS-PAGE gels, and immunoblotted, and bands were quantified by scanning densitometry.

Mass Spectrometry

Collagen bead–bound proteins were isolated from cells. Dishes (10 cm; three for each treatment) were washed with PBS to remove unbound beads. Cells were scraped into cytoskeletal isolation buffer (200 μl; CSKB; 1% Triton X-100, 50 mM NaCl, 300 mM sucrose, 3 mM $MgCl_2$, 0.5 mM EGTA, 20 μg/ml aprotinin, 1 μg/ml Pefabloc, and 10 mM Pipes, pH 6.8, containing protease inhibitors). Pooled samples from three dishes were sonicated on ice and centrifuged to collect the beads, which were washed with CSKB and with 25 mM NH_4HCO_3. Beads were suspended in 300 μl of 25 mM NH_4HCO_3 containing 1 μg trypsin (Roche, Indianapolis, IN) and rotated overnight at 37°C. Supernatants were combined with 0.1% trifluoroacetic acid, and samples were dried. Lyophilized samples were analyzed by MALDI with an Applied Biosystems Voyager-DE STR MALDI-time of flight mass spectrometer (Foster City, CA; 337-nm laser; Mass Spectrometry Facility, Hospital for Sick Children, Toronto). Data from the LCMS runs were analyzed using the National Center for Biotechnology Information (NCBI) database and the MASCOT search engine. MOWSE (molecular weight search) scores, assigned by MASCOT, were calculated as described (Pappin *et al.*, 1993).

In Vitro Binding Analyses

Proteins expressed in bacterial expression systems were isolated and purified as described previously (Li *et al.*, 2003; Garrett *et al.*, 2008). Protein concentrations were determined by running standards on SDS polyacrylamide gels or by the bicinchoninic acid protein determination method.

To assess binding of NM II-A rod filaments (residues 1338–1960) to GST-Rap1A, proteins were dialyzed against assembly buffer (20 mM Tris, pH 7.5, 20 mM NaCl, 2 mM $MgCl_2$, 1 mM DTT) overnight before binding assays.

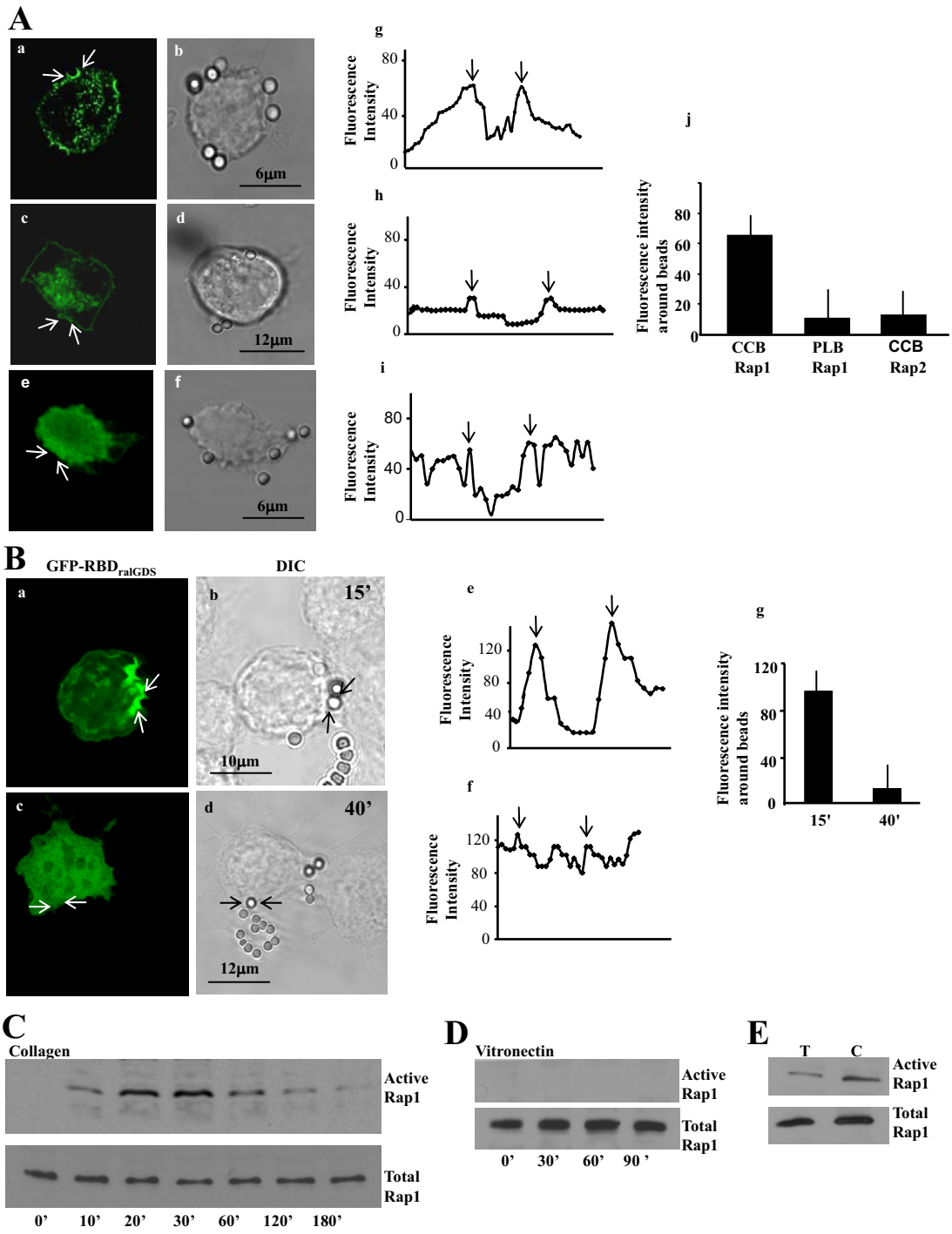

Figure 1. (A) Localization of GFP-Rap1 in fibroblasts treated with collagen-coated beads (CCB) (a and b) or poly-L-lysine (PLB) beads (c and d), or localization of Rap2 in fibroblasts treated with CCB (e and f). Confocal microscopy line scans of fluorescence intensities across beads showed a >3-fold accumulation of Rap1 around collagen beads compared with poly-L-lysine–coated beads or Rap2 around collagen beads (Figure 1A, g–i). The graphs (g–i) show fluorescence intensity line scans across bead sites marked by the arrows in panels a, c, and e. The arrows in the graphs (g–i) show the point of intersection with beads. Data from 25 separate line scans from three independent experiments is quantified in the histogram (j; mean ± SEM; CCB for Rap1 was larger than PLB or Rap2; $p < 0.01$). (B) Localization of active Rap1 in fibroblasts treated with collagen-coated beads. GFP-RBD of RalGDS, which binds active Rap1, localized to collagen beads at early times of incubation (a and b), but was diffusely distributed throughout the cell by 40 min after collagen bead incubation (c and d). Fluorescence intensity line scans (e and f) at the bead site marked by arrows in panels a and c. The arrows in graphs e and f show the point of intersection with beads. The histograms g and j show the fluorescence intensity (mean ± SEM) from three independent experiments, 25 cells per experiment. (C and D) A pulldown assay with GST-RalGDS to determine levels of GTP-bound Rap1 associated with collagen or vitronectin beads. Data shown are representative of three independent experiments. (E) Cells incubated with $\alpha 2\beta 1$-blocking antibody (T) or with control antibody (C) were stimulated with collagen beads, and active Rap1 was determined by immunoblotting of RalGDS-binding proteins. This experiment was repeated three times with similar results.

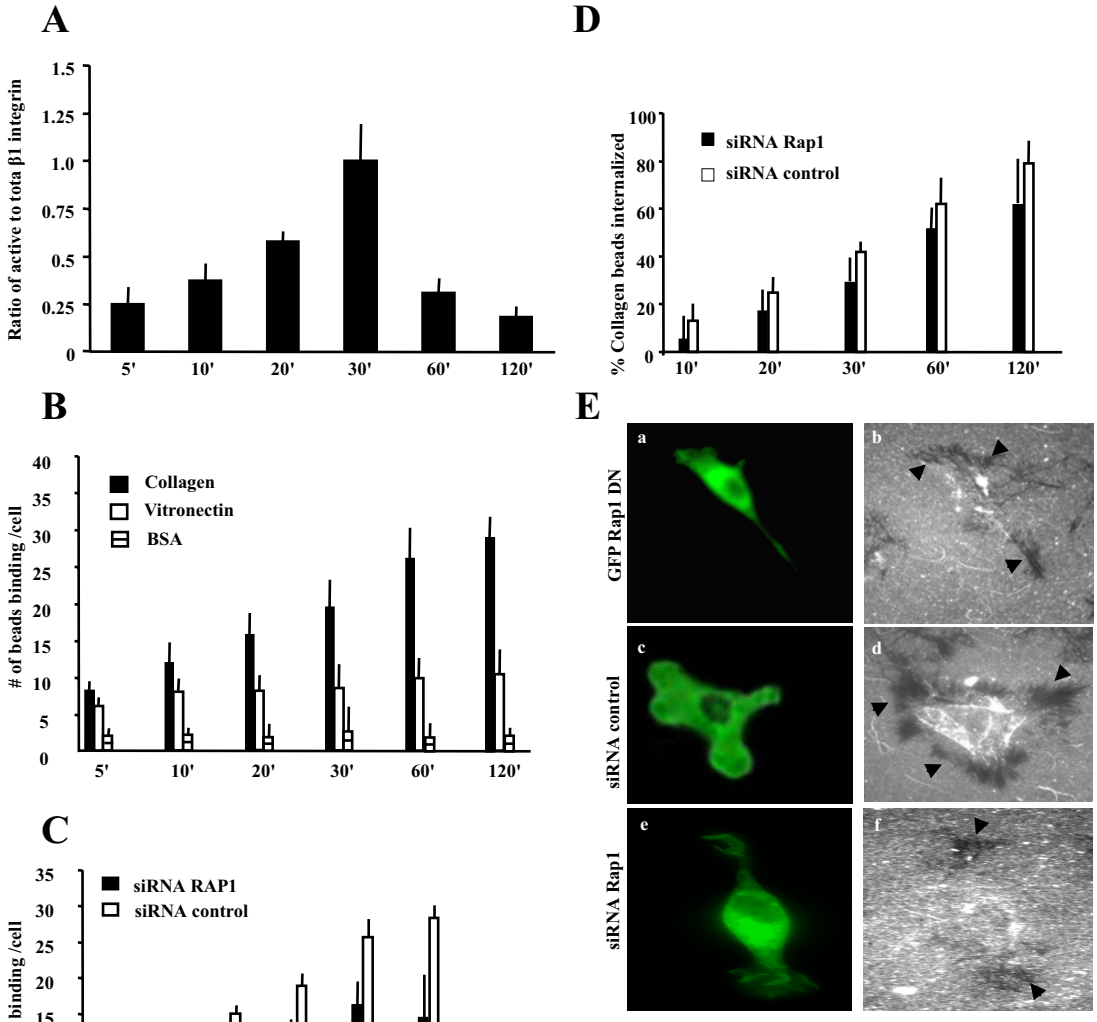

Figure 2. (A) For microscopic observations, cells were incubated with collagen-coated beads for different lengths of time, fixed, and stained for activated β1-integrin (mAb; clone 9EG7) and total β1-integrin (KMI6). The histogram shows the ratio of fluorescence intensities around the beads of active β1-integrin to total β1-integrin (mean ± SEM). (B) Collagen-coated beads showed progressive increases in binding over 120 min compared with vitronectin or BSA-coated beads. (C and D) Rap1-deficient cells exhibit reduced collagen-bead binding and bead internalization compared with cells treated with control siRNA. (E) Collagen uptake in cells expressing GFP-Rap1 DN (a and b), and transfected with fluorescently labeled control (c and d) or c Rap1 (e and f) siRNA after 4 h. Cells treated with control siRNA show substantial clearance of fluorescent collagen (black arrows in d) compared with Rap1 knockdown cells (f) or cells expressing dominant negative (DN) Rap1 (b). (A–D) The data represent mean ± SEM for three independent experiments, 25 cells per experiment.

Varying concentrations of purified GST-Rap1A (3–12 μM) were incubated with assembled NM II-A rods (8 μM) at 23°C for 45 min. Samples were centrifuged for 15 min at 80,000 rpm. Supernatant and pellet samples were separated by SDS-PAGE and stained with Coomassie blue. Similar experiments were done with GST-Rap2 bound to glutathione-Sepharose and GST bound to glutathione-Sepharose beads.

We determined if interactions between GST-Rap1 and NM II-A were GDP- or GTP-dependent (Jeong *et al.*, 2007). GST-Rap1 was incubated in buffer (50 mM Tris, pH 7.4, 1 mM EDTA, 20 mM NaCl, 1% Triton X-100) for 10 min at room temperature followed by the addition of 140 μM GTPγS or GDP. After 30 min, samples were precleared with 50 μl glutathione-Sepharose before incubation with assembled NM II-A rods in filament assembly buffer.

Immunofluorescence and Confocal Microscopy

We determined the distribution of Rap1 or myosin II isoforms. Cells were incubated with beads, fixed with 3% formaldehyde in PBS, permeabilized with 0.2% Triton X-100, and stained. For in situ permeabilization assays, cells transfected with GFP- NM II-A were washed with cold PBS followed by 1 min of extraction with ice-cold permeabilization buffer containing 10 mM Tris, pH 7.0, 60 mM KCl, 125 mM sucrose, and 0.05% Triton X-100. Cells were washed three times in cold wash buffer containing 10 mM Tris, pH 7.0, 30 mM KCl, 5 mM $MgCl_2$, and fixed for 8 min in buffer containing 3.7% formaldehyde in cytoskeleton stabilization buffer (137 mM NaCl, 5 mM KCl, 1.1 mM Na_2HPO_4, 2 mM $MgCl_2$, 2 mM EGTA, 5 mM PIPES, and 5.5 mM glucose, pH 6.1; Small, 1981). Cells were stained with rhodamine phalloidin for actin filaments.

The spatial distribution of staining around beads was determined by confocal microscopy (Leica, Heidelberg, Germany; 40 × oil immersion lens). Transverse optical sections were obtained at 0.5-μm nominal thickness using Leica software and analyzed with Adobe Photoshop (San Jose, CA). Colocalization was analyzed three to six fields per cell, depending on the number of bound beads by using the ImageJ plug-in JACoP (http://rsb.info.nih.gov/ij/; Bolte and Cordelieres, 2006). The Pearson's r was expressed as the mean ± SD. For intensity analysis of fluorescence around beads, cells in confocal microscopic fields were selected randomly. An optical section with the most beads in maximal focus was selected for intensity quantification; beads that were out of focus were not included. Leica confocal software was used to measure pixel intensity along the line scans at the bead site. Maximal fluorescence intensity (represented as intensity peaks in a line scan) was sub-

Table 1. LC-MS/MS analysis of bead-associated proteins

Name of protein	Accession no.	MOWSE score
Myosin	NP_037326	400
Vimentin	NP_112402	282
Actin	ATRTC	104
Histone H2A.1	PO2262	344
Histone H1 d	JH0159	190
Histone H2B	0506206A	172
GAPDH	P04797	220
Tublin α	0812252A	117
Tublin β	NP-035785	105
Laim B1	NP-446357	136
Collagen α1	CAB01633	156

tracted from the basal cell cytoplasmic fluorescence intensities close to the region of interest but not within the immediate vicinity of the bead.

Small Interfering RNA and Transfections

Cells (10^5–10^7) growing in tissue culture plates were transfected with 5–20 pmol of Smart Pool small interfering RNA (siRNA) oligonucleotides specific to MLCK, Rap1, NM II-A, or NM II-B (Dharmacon Research, Boulder, CO) using Oligofectamine (Invitrogen, Carlsbad, CA) without antibiotics. Cells were transfected with dominant negative GFP-Rap1 using FuGENE6 transfection reagent (Roche). After titration experiments for optimizing vector concentration, cells were transfected, incubated for 48 h, and subjected to substrate clearance assays. To estimate transfection efficiency and to serve as a transfection control, pEGFPluc (Clontech, Palo Alto, CA) was used, and the number of fluorescent cells were counted.

Statistical Analyses

For continuous variables, means and SEs of means were computed and are displayed in *Results*. Differences between groups were evaluated by Student's unpaired *t* test or ANOVA for multiple comparisons. Statistical significance was set at $p < 0.05$. Post hoc comparisons were performed with Tukey's test. For all experiments, at least three independent experiments were evaluated, each performed in triplicate.

RESULTS

Rap1 Localizes to Collagen-coated Beads

Because Rap can regulate spreading, cell adhesion and phagocytosis in mammalian neutrophils and macrophages (Seastone *et al.*, 1999; Reedquist *et al.*, 2000; Arthur *et al.*, 2004; Bivona *et al.*, 2004), we examined whether Rap is involved in the binding step of collagen phagocytosis. In mouse fibroblasts incubated with collagen-coated latex beads, GFP-Rap1 was enriched around collagen beads after 20 min of incubation with cells (Figure 1A, a and b) but not around poly-L-lysine–coated beads (Figure 1A, c and d). We also observed localization of endogenous Rap1 to beads (not shown), but Rap2 did not localize to cups at collagen bead sites (Figure 1A, e and f). Line scans of fluorescence intensities through bead bound areas showed a more than threefold accumulation of Rap1 around collagen beads compared with poly-L-lysine–coated beads or Rap2 around collagen beads (Figure 1A, g–j).

Table 2. A. LC-MS/MS analysis of Rap1A immunoprecipitates

	No. of peptides	
Name of protein	Untreated	Collagen bead treated
NMHC II-A	1	17
Actin	1	6
Histone H1.3	2	4
Keratin II	2	2
Vimentin	1	2
Histone	1	2
NMHC II-B	2	5
Myosin light chain	0	2

Table 3. Sequence identification for NMHC II-A and NMHC II-B peptides from collagen bead–induced samples

NMHC II-A	NMHC II-B
IMGIPEDEQMGLLR	LVQEQGSHSK
VISGVLQLGNIAFK	NTNPNFVR
VSHLLGINVTDFTR	AGVLAHLEEER
NTNPNFVR	KFDQLLAEEK
AGVLAHLEEER	VLAYDKLEK
RQQQLTAMK	
HEDELLAK	
KEEELQAALAR	
THEAQIQEMR	
KVEAQLQELQVK	
KFDQLLAEEK	
ALEEAMEQK	
DLEAHIDTANK	
ASREEILAQAK	
DELADEIANSSGK	
NAEQFKDQADK	
RGDLPFVVTR	

Peptides were analyzed by peptide mass fingerprinting and matched to predicted sequences.

Temporal Activation of Rap1 in Response to Collagen-Bead Binding

We determined whether Rap1 localized to collagen beads was in a GTP-bound state. GFP-tagged RBD of RalGDS was used to specifically detect active Rap1. Transfected cells exhibited enhanced RBD_{RalGDS} fluorescence at the cell periphery; this staining was localized prominently to beads at early time points (15 min; Figure 1B, a and b). By 40 min after collagen-bead binding the staining was diffusely distributed throughout the cell (Figure 1B, c and d). Line scans of fluorescence intensities through bead-bound areas showed significantly higher fluorescence around collagen beads at 15 min than at 40 min (Figure 1B, e–g).

Rap1 can activate collagen receptors and thereby increase cell binding to matrix ligands via β1-integrins (Bos *et al.*, 2001), but it is not known if β1-integrin ligation can activate Rap1. We conducted pulldown assays using GST-RalGDS fusion protein to estimate levels of GTP-bound Rap1 in cells stimulated with collagen or vitronectin-coated beads. Vitronectin, which is bound by β3-integrins, was used as a control. Triton-soluble proteins were isolated from fractions of bead-associated cytoskeletal membranes at various times after incubation with beads. There was no detectable GTP-bound Rap1 in cells incubated with vitronectin beads, whereas collagen beads induced a time-dependent increase in Rap1 activity, which peaked at 30 min (Figure 1, C and D; Supplementary Figure S1a).

We determined the importance of the $\alpha2\beta1$-integrin in Rap1 activation with the use of an $\alpha2\beta1$-blocking antibody or an irrelevant isotype control antibody that was coincubated with collagen beads. In samples incubated with the $\alpha2\beta1$-blocking antibody, although the cells bound to the beads, there was approximately a fourfold reduction in Rap 1 activity compared with samples treated with the control antibody (Figure 1E; Supplementary Figure S1b).

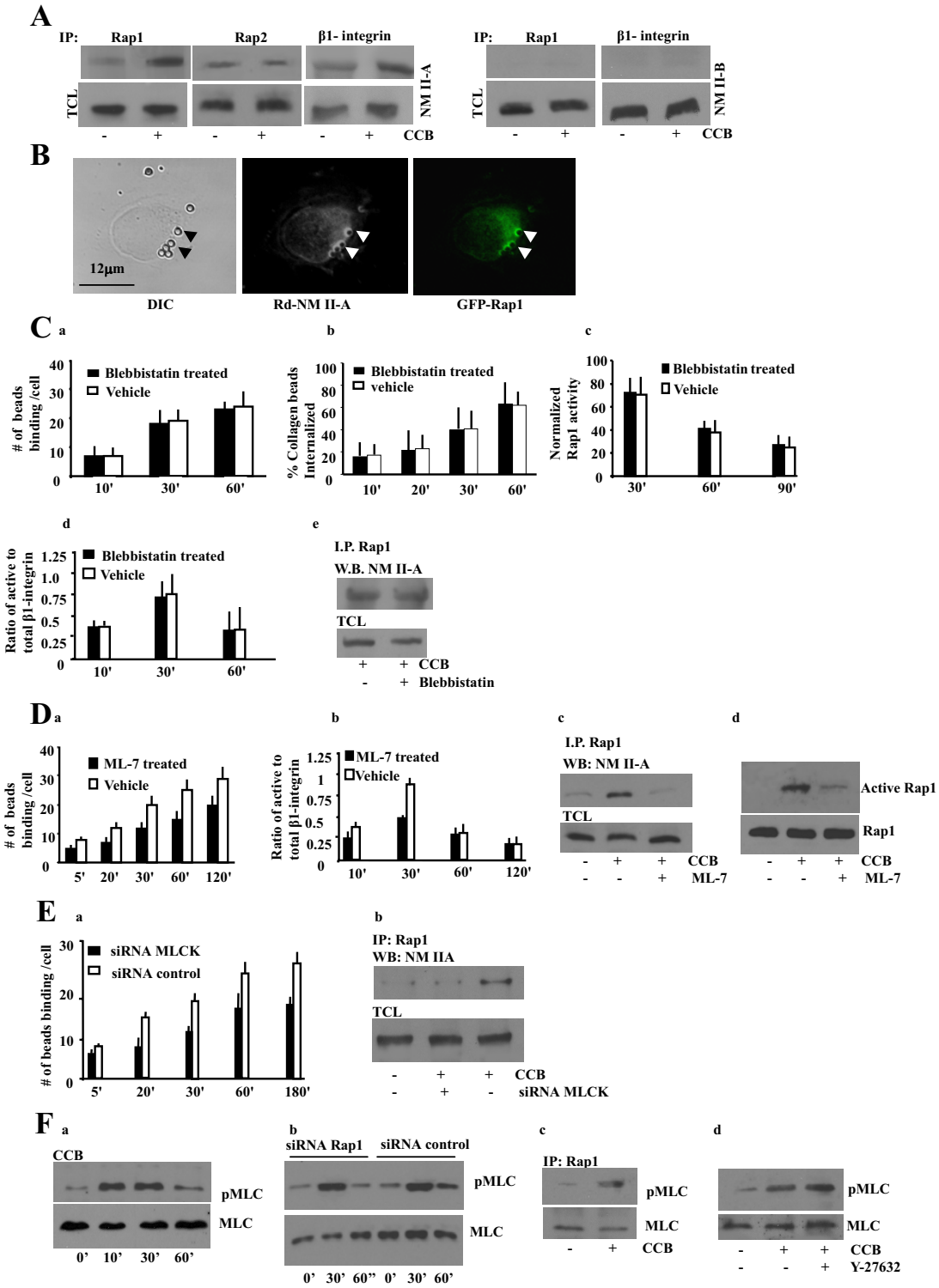

Figure 3. (A) Cells were incubated with collagen coated beads (CCB; +) or not (−). Rap1, Rap2, or β1-integrin immunoprecipitates of bead-associated proteins were immunoblotted for NM II-A or NM II-B. TCL, total cell lysates. (B) Colocalization of NM II-A and GFP-Rap1 at bead sites. The overlay shows close spatial association of Rap1 and NM II-A at bead sites. (C, a and b) Fibroblasts treated with vehicle or 25 μM blebbistatin exhibit similar collagen-bead binding and collagen-bead internalization. Similar results were obtained with 50 or 100 μM blebbistatin. (c–e) Cells incubated with 25 μM blebbistatin did not effect collagen-induced Rap1 activity, β1-integrin activation, or Rap1 interaction with NM II-A. (D) (a) ML-7– treated (25 μM) fibroblasts show reduced collagen-bead binding ($p < 0.01$ after 5 min). (b) Ratio of active to total β1-integrin around collagen beads in ML-7 and vehicle-treated cells. ML-7 disrupts the interaction of NM II-A with Rap1. (c) Rap1 immunoprecipitates in presence or absence of ML-7 treatment, and collagen induced samples were probed with NM II-A antibody. CCB, collagen-coated beads; TCL, total cell lysate. (d) Pulldown assays using GST-RalGDS to evaluate the effect of ML-7 treatment on Rap1 activity in cells stimulated with collagen. (E) (a) MLCK knockdown cells exhibit reduced collagen-bead binding ($p < 0.01$ after 5 min). (b) Rap1 immunoprecipitates were isolated from cells transfected with siRNA to MLCK after previous incubation with collagen beads (30 min).

Activation of β1-integrin in Response to Collagen-Bead Binding

Because Rap1 can activate β1-integrins (Bos *et al.,* 2003), we asked whether Rap1 activity may increase the activity of preexisting cell surface integrins or enhance expression of cell surface integrins. Fibroblasts were stimulated with collagen beads and immunostained with an antibody that detects activated β1-integrin (clone 9EG7). To estimate total (active and inactive) β1-integrin surface expression in cells, nonfixed viable cells were incubated with labeled β1-integrin antibody (KMI6), and the fluorescence around the collagen beads was measured. The level of active β1-integrin around collagen beads peaked at 30 min; however, there was no change in surface expression of total β1-integrin at bead sites over the same time period (Figure 2A). We examined the binding of vitronectin-coated beads, which use β3-integrins for cell attachment, and BSA-coated beads, which represent a nonintegrin dependent protein interaction. The number of bound collagen-coated beads increased over time (5–120 min; Figure 2B). The binding of vitronectin and BSA-coated beads was a small fraction of collagen-bead binding and did not substantially increase over time. Although β1-integrin activation increased markedly up to 30 min after bead addition, increased bead binding continued up to 120 min, suggesting that other collagen adhesion–promoting molecules such as endo180 (Curino *et al.,* 2005) may play a role in the later stages of collagen phagocytosis. It is also possible that Rap1 activation is an early step in the process of enhanced bead binding (affinity change), after which Rap1 may get inactivated, but the process continues with a Rap-independent second phase.

Next we tested whether Rap is important for collagen phagocytosis. Knockdown of Rap1 with siRNA treatment reduced Rap1 protein levels by 70% after 36 h compared with a nontargeted siRNA, untreated cells, or cells treated with transfection reagent alone (Supplementary Figure S2). Cells transfected with siRNA for Rap1 or nontargeted siRNA both showed a gradual increase in collagen-bead binding. However, Rap1 knockdown cells showed a significant reduction in bead binding from 20 min onward compared with Rap1-expressing cells ($p < 0.05$). At 120 min Rap1 knockdown cells exhibited a 50% reduction in bead binding ($p < 0.01$; Figure 2C).

To evaluate the role of Rap1 in collagen-bead internalization, we measured the percent of internalized beads as a function of beads bound to cells. There was no significant difference between control and Rap1 knockdown cells ($p > 0.2$; Figure 2D), indicating that Rap1 affected the binding but not the subsequent internalization step of phagocytosis. We also examined the binding and internalization of fluorescently labeled collagen in Rap1 knockdown cells, siRNA control cells, or cells expressing a dominant negative Rap1. Cells expressing a GFP-tagged dominant negative Rap1 (Figure 2E, a and b) or treated with Rap1-specific siRNA (Figure 2E, e and f) exhibited low or no measurable collagen clearance, which appears as dark areas around the cell, compared with cells transfected with a nontargeted siRNA (Figure 2E, c and d). Taken together, these observations indicate that Rap1 is required for collagen binding and that the subsequent effects of Rap inhibition on collagen internalization are due to the initially reduced binding of cells to collagen.

Because previous data have indicated that the stiffness of the phagocytic target can affect internalization and that contractility can contribute to these processes (Beningo and Wang, 2002), we incubated cells on stiff or soft collagen substrates (Arora *et al.,* 1999). There was 25% higher internalization with the softer substrates (FITC-collagen signals in flow cytometry fluorescence units: stiff = 3.0 ± 0.2; soft = 4.1 ± 0.3; $p > 0.05$), indicating a modest effect of substrate stiffness on internalization.

Rap1 Interacts with NM II-A

We identified proteins involved in targeting Rap1 to collagen-binding sites after integrin-mediated collagen ligation. Collagen bead–associated proteins were analyzed by tandem mass spectrometry. Several identified proteins (e.g., NMHC II-A, vimentin, and β-actin) had high MOWSE scores (Table 1), indicating that these proteins were associated with the adhesion complex associated with collagen beads. We next used tandem mass spectrometry to identify Rap1-interacting proteins. Rap1 was immunoprecipitated from cells incubated with collagen beads or from untreated cells, and the immunoprecipitates were analyzed by MALDI. Of the proteins that bound to Rap1 (Table 2), the MOWSE scores were highest for NMHC II-A. The peptides obtained by MALDI analysis were used to search the NCBI database; 17 tryptic peptides matched sequences in the mouse NMHC II-A. Another five peptides matched sequences in mouse NMHC II-B (Table 3). As these differences in the number of peptides detected may have indicated higher overall abundance of NHMC II-A, we also examined whole cell lysates by mass spectrometry. At 95% confidence limits (by MOWSE), we found 96 peptides for NMHC II-A and 44 peptides for NMHC II-B.

Immunoblotting of Rap1 immunoprecipitates was used to verify the association of NMHC II-A and II-B with Rap1. Rap1 immunoprecipitates from collagen bead–treated cells exhibited a 3.5-fold increase in NMHC II-A compared with immunoprecipitates from untreated cells (Figure 3A; $p < 0.05$; Supplementary Figure S3a). In contrast, Rap2 immunoprecipitates did not show an increase in NM II-A in response to collagen beads. NMHC II-B was not detected in Rap1 immunoprecipitates from collagen bead–stimulated and unstimulated cells (Figure 3A). Because NM II-A associated with Rap1 and Rap1 can regulate β1-integrin activity (Bos, 2005), we asked if NM II-A coprecipitated with β1-integrin (Figure 3A). β1-integrin immunoprecipitates showed only a small increase (1.5-fold) in NM II-A after incubation with collagen beads compared with untreated cells. There was no detectable NM II-B immunoprecipitated with Rap1 or β1-integrin in these samples (Figure 3A). ***

We assessed the spatial relationship between Rap1 and NM II-A. GFP-Rap1–transfected cells were treated with collagen beads and immunostained for NM II-A. There was a high degree of overlap between the two fluorescent signals at bead sites (Pearson's r = 0.893 ± 0.08). Within the cytoplasm there was very little signal overlap (Pearson's coefficient = 0.268 ± 0.06), suggesting that colocalization of Rap1 and NM II-A is restricted primarily to collagen bead sites (Figure 3B).

We determined if NM II-A motor activity was involved in the early stages of collagen bead attachment by treating cells

figure 3 (cont). Blots were probed for NM II-A. For C, a and b; D, a and b; and E, panel a, data represent the mean ± SEM for three independent experiments, 25 cells per experiment. (F) (a) Bead-associated proteins collected from cells induced with collagen-coated beads show maximal phosphorylation of MLC at 30 min. (b) Cells transfected with Rap1 siRNA show similar MLC phosphorylation during incubation with collagen-coated beads as siRNA controls. (c) Rap1 immunoprecipitates interacted with phospho-MLC in response to collagen-bead binding. (d) Treatment with Rho kinase inhibitor (Y-27632; 10 μM) does not effect phosphorylation of MLC in response to collagen binding.

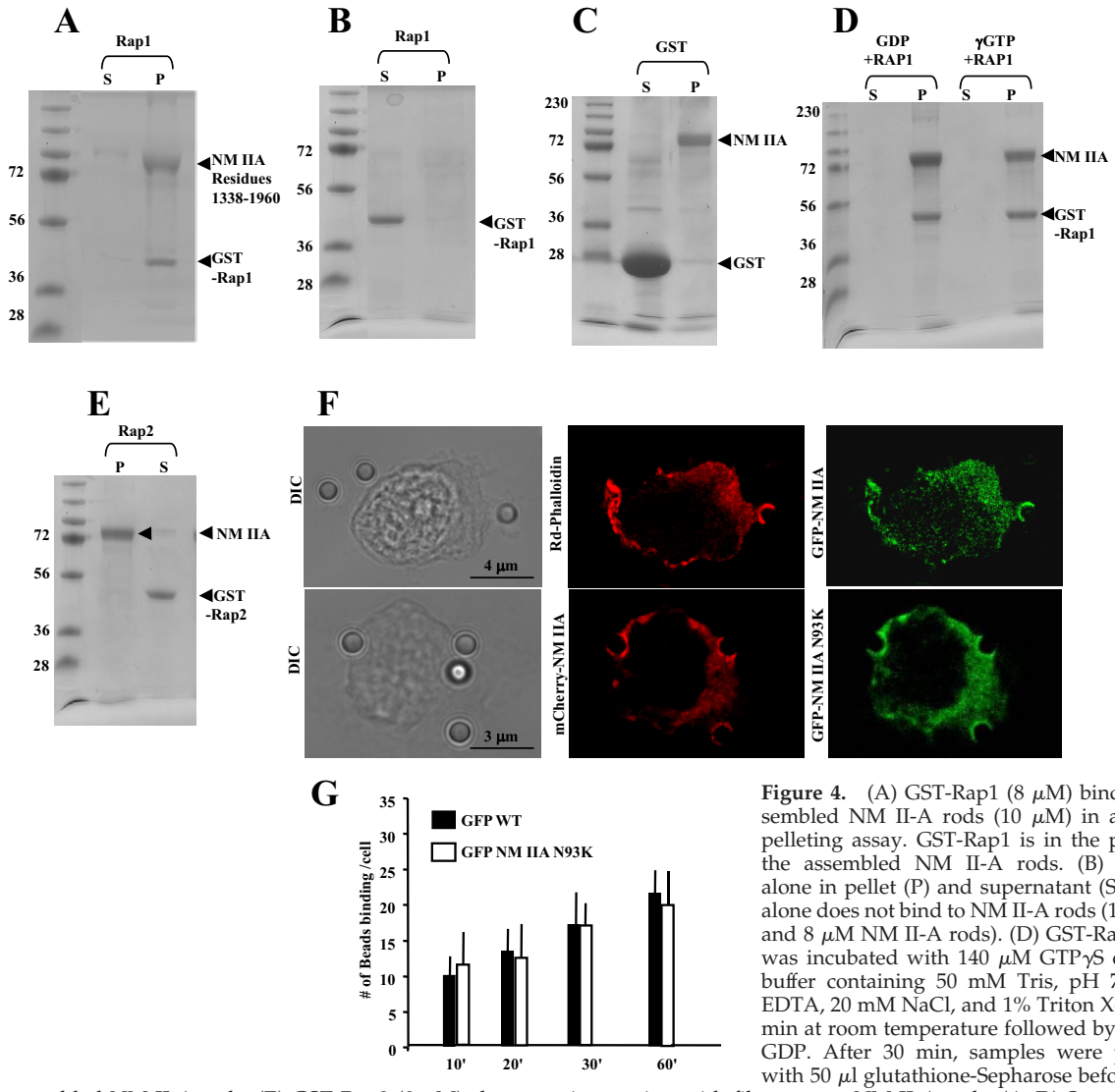

Figure 4. (A) GST-Rap1 (8 μM) binding to assembled NM II-A rods (10 μM) in a standard pelleting assay. GST-Rap1 is in the pellet with the assembled NM II-A rods. (B) GST-Rap1 alone in pellet (P) and supernatant (S). (C) GST alone does not bind to NM II-A rods (12 μM GST and 8 μM NM II-A rods). (D) GST-Rap1 (8 μM) was incubated with 140 μM GTPγS or GDP in buffer containing 50 mM Tris, pH 7.4, 1 mM EDTA, 20 mM NaCl, and 1% Triton X-100 for 10 min at room temperature followed by GTPγS or GDP. After 30 min, samples were precleared with 50 μl glutathione-Sepharose before incubation with assembled NM II-A rods. (E) GST-Rap2 (8 μM) shows no interaction with filamentous NM II-A rods. (A–D) S, supernatant; P, pellet. (F) Top panel, representative images showing distribution of GFP-NM II-A filaments and F-actin after Triton permeabilization. A total of 20 cells were examined. Bottom panel: Images show colocalization of WT mCherry-NM II-A with N93KGFP-NM II-A mutant lacking motor activity in Triton-permeabilized cells. (G) There was no difference in collagen-bead binding in cells transfected with WT GFP -NM II-A or GFP NM II-A N93K.

with blebbistatin and measuring bead binding. There was no difference in the number of bound beads in blebbistatin-treated cells compared with vehicle-treated cells (Figure 3Ca). Blebbistatin also had no effect on collagen bead internalization, collagen-induced Rap1 activity, the activation state of the β1-integrin, or interactions between Rap1 and NM II-A (Figure 3C, b–e). In contrast, treatment with the MLCK inhibitor ML-7 caused a reduction in collagen-bead binding ($p < 0.05$ after 5 min), suggesting the involvement of MLC phosphorylation in this process (Figure 3Da). We examined whether the high-affinity state of the β1-integrins (as detected by the 9EG7 antibody) was affected by inhibition of MLC phosphorylation. Fibroblasts treated with ML-7 (25 μM) showed reduced fluorescence intensity at collagen bead sites compared with untreated cells, suggesting that the regulation of integrin affinity depends, in part, on phosphorylation of the MLC (Figure 3Db). The interaction between Rap1 and NM II-A and collagen bead–induced Rap1 activation were inhibited by ML-7 (Figure 3D, c and d). Treatment with ML-7 (25 μM) significantly inhibited collagen-induced phosphorylation of MLC (Supplementary Figure S3b). To confirm the involvement of MLCK, we used siRNA to reduce MLCK protein expression. Cells transfected with MLCK siRNA showed a 70–80% reduction in MLCK levels as evaluated by densitometry (Supplementary Figure S3c). MLCK knockdown reduced collagen binding ($p < 0.01$ after 5 min) and the interaction between Rap1 and NM II-A (Figure 3E, a and b).

To determine whether collagen-bead binding correlates temporally with myosin II phosphorylation at collagen bead sites, we used a phospho-MLC antibody to evaluate the phosphorylation status of NM II. These data showed a time-dependent increase of MLC phosphorylation, which peaked between 10 and 30 min. (Figure 3Fa). Rap1 knockdown did not affect MLC phosphorylation, suggesting that Rap1 is not required for integrin-induced myosin II phosphorylation (Figure 3Fb). As a control, fibroblasts were treated with ionomycin (2 μM) to increase $[Ca^{2+}]_i$, and these cells

showed robust MLC phosphorylation (Supplementary Figure S3d). However, collagen-bead binding did enhance the interaction of Rap1 with phosphorylated MLC (Figure 3Fc). Treatment with the Rho kinase inhibitor (Y-27632) showed no effect on collagen-induced MLC phosphorylation (Figure 3Fd) or on collagen-bead binding to cells (60 min: treated cell = 18 ± 3.2 beads per cell; untreated cells = 20 ± 4.5 beads per cell; $p > 0.2$).

Interaction between Rap1A and NM II-A

To evaluate the direct interaction of Rap1 and NM II-A, we examined the binding of Rap1A to assembled myosin II-A rods (residues 1338–1960) in a cosedimentation assay. GST-Rap1 was detected in pellets after high-speed sedimentation (Figure 4A), but GST Rap1 by itself did not aggregate in the sedimentation buffer and remained in the supernatant (Figure 4B). GST alone did not bind NM II-A rods (Figure 4C). In addition the binding of Rap1 to NM II-A was independent of nucleotide state of Rap1 (Figure 4D). Similar experiments were performed with Rap2-GST, which showed a negligible amount of interaction with NM II-A filamentous rods (Figure 4E).

Our data showed that although blebbistatin failed to inhibit bead binding, MLC phosphorylation was required for enhanced bead binding. Because MLC phosphorylation activates the myosin II motor and promotes filament assembly (Watanabe *et al.*, 2007), these observations suggest that with respect to bead binding the role of MLC phosphorylation may be to enhance filament assembly. To separate these two aspects of MLC-mediated regulation of myosin II function and determine if MLC phosphorylation enhances NM II-A filament assembly and association with actin at collagen bead sites, cells transfected with WT GFP-NM II-A were permeabilized with Triton to release unassembled NM II-A. There was colocalization of actin filaments and NM II-A at bead-binding sites (Figure 4E). In addition, GFP-NM II-A N93K, which is largely defective in motor activity (Hu *et al.*, 2002), but can assemble into filaments (Vicente-Manzanares *et al.*, 2007), localizes to collagen-bead binding sites in a comparable manner to WT mCherry-NM II-A (Figure 4E). Further we found no difference in collagen-bead binding in cells transfected with Wt or the motor-deficient mutant NM II-A N93K (Figure 4G).

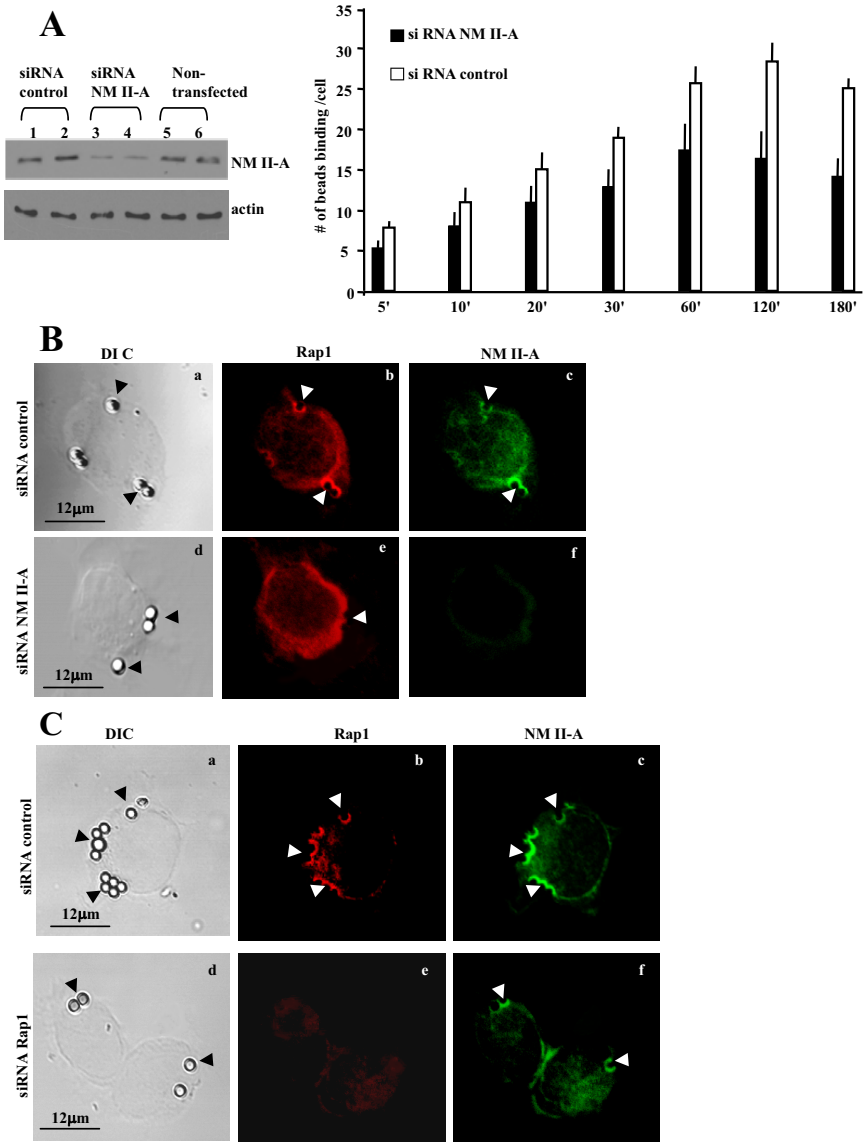

Figure 5. (A) 3T3 fibroblasts transfected with NM II-A siRNA show a 70% reduction in NM II-A protein levels compared with cells treated with nontargeted siRNA. NM II-A knockdown cells exhibit reduced numbers of bound collagen beads compared with control cells ($p < 0.05$ after 20 min; 25 cells per time point). (B) Cells transfected with siRNA for NM II-A do not show Rap1 localization to collagen beads (compare b and e). (C) Knockdown of Rap1 reduces collagen-bead binding, but NM II-A still localizes to collagen beads (compare c and f).

Requirement for NM II-A for Collagen-Bead Binding

We used siRNA to knock down NM II-A in mouse fibroblasts. Protein levels of NM II-A were reduced by ~70% (Figure 5A, left). NM II-A knockdown cells showed reduced bead binding (Figure 5A, right; 50% reduction at 120 min; $p < 0.02$), whereas in control cells collagen-bead binding increased gradually over time (5–120 min). Immunostaining showed NM II-A knockdown inhibited localization of Rap1 to collagen beads (Figure 5B, d–f), whereas in Rap1 knockdown cells, NM II-A localized to collagen beads in a similar manner to control cells (Figure 5C, d–f). Cells treated with control siRNA showed colocalization of Rap1 and NM II-A.

Regulation of Rap1 by NM II-A

The role of NM II-A in the regulation of Rap1 and collagen binding was examined using NM II-A and NM II-B null embryonic (ES) cells (Conti *et al.*, 2004). Immunoblot analysis indicated that WT, NM II-A null and NM II-B null ES cells express equivalent amounts of β1-integrin, Rap1, Rap2, and β-actin (Figure 6A). As observed in fibroblasts, WT cells

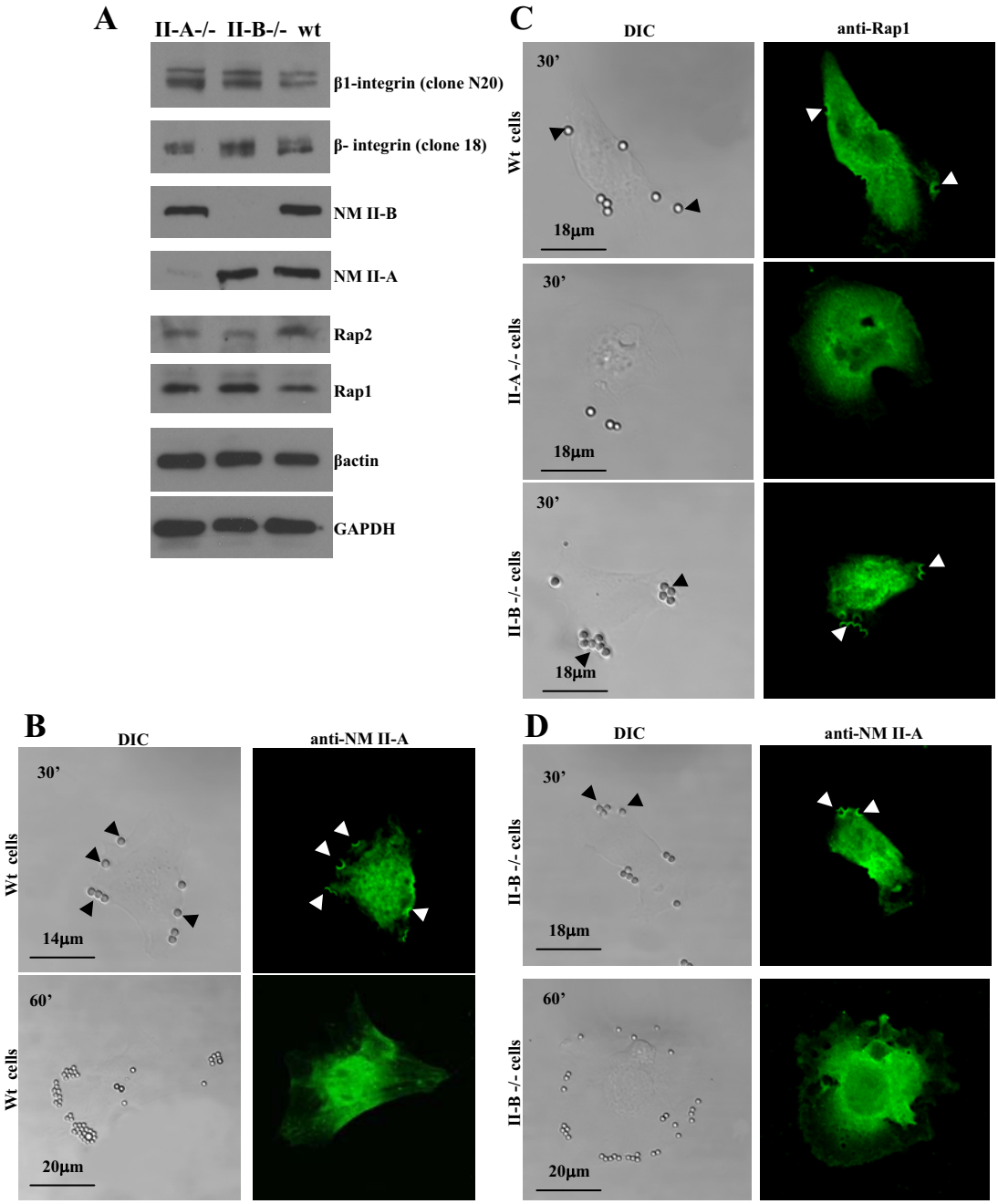

Figure 6. (A) Total cell lysates from NM II-A null, NM II-B null, and wild-type (Wt) ES cells were immunoblotted for the indicated proteins. (B) Immunostained WT cells show accumulation of NM II-A in phagocytic cups at bead-binding sites at 30 min. By 60 min, NM II-A staining at bead sites disappeared. (C) WT cells and NM II-B null cells showed accumulation of Rap1 at bead sites after 30-min incubation, but the absence of NM II-A prevented localization of Rap1 to beads. (D) In NM II-B null cells, NM II-A localizes to beads at 30 min and is absent at 60 min.

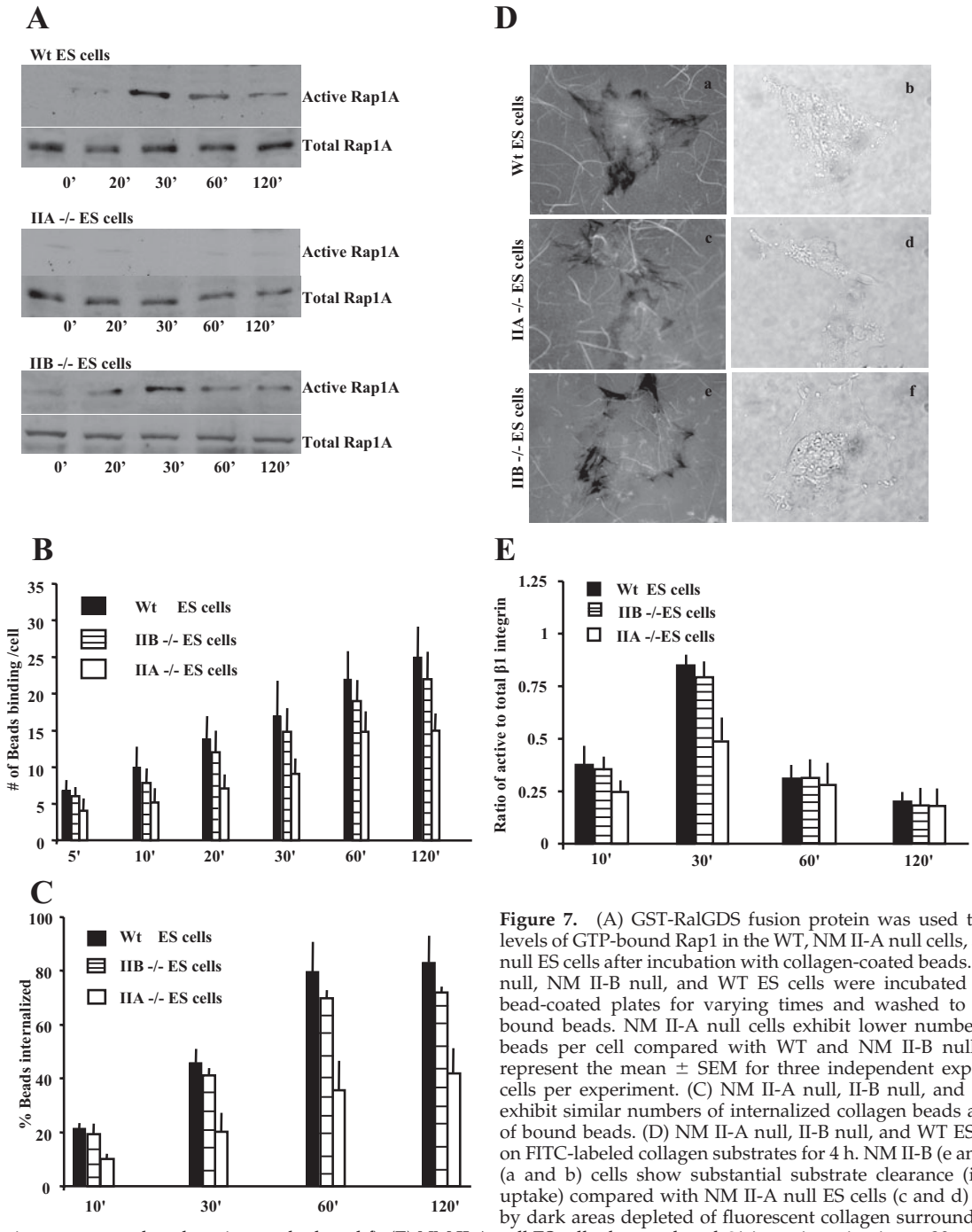

Figure 7. (A) GST-RalGDS fusion protein was used to determine levels of GTP-bound Rap1 in the WT, NM II-A null cells, and NM II-B null ES cells after incubation with collagen-coated beads. (B) NM II-A null, NM II-B null, and WT ES cells were incubated on collagen bead-coated plates for varying times and washed to remove unbound beads. NM II-A null cells exhibit lower numbers of bound beads per cell compared with WT and NM II-B null cells. Data represent the mean ± SEM for three independent experiments, 25 cells per experiment. (C) NM II-A null, II-B null, and WT ES cells exhibit similar numbers of internalized collagen beads as a function of bound beads. (D) NM II-A null, II-B null, and WT ES cells plated on FITC-labeled collagen substrates for 4 h. NM II-B (e and f) and WT (a and b) cells show substantial substrate clearance (i.e., collagen uptake) compared with NM II-A null ES cells (c and d) as indicated by dark areas depleted of fluorescent collagen surrounding the cells (fluorescence images a, c, and e; phase images b, d, and f). (E) NM II-A null ES cells show reduced β1-integrin activation at 30 min compared with NM II-B and WT ES cells.

showed accumulation of NM II-A in phagocytic cups at collagen-bead binding sites, which disappeared by 60 min, probably because the majority of the beads were internalized (Figure 6B). In contrast, NM II-A null cells bound fewer beads and Rap1 did not localize to bead-binding sites (Figure 6C). In NM II-B null cells, Rap1, and NM II-A localized to beads, similar to WT cells (Figure 6D).

After collagen-bead binding, GTP-bound Rap1 was not detected in NM II-A null cells compared with WT or II-B null cells (Figure 7A; Supplementary Figure S4). At 30 min, collagen-bead binding was reduced in NM II-A null cells by 50% compared with WT and NM II-B null cells ($p < 0.01$; Figure 7B). Internalization of the bound beads depended on the expression of NM II-A (Figure 7C). An examination of collagen uptake demonstrated that WT and NM II-B null cells exhibited measurable collagen clearance compared with NM II-A null cells (Figure 7D, a–f). These observations suggest that interactions between Rap1 and NM II-A are required for collagen binding and are a rate-limiting step for collagen internalization. Because we observed that Rap1 regulated β1-integrin affinity, we examined whether β1-integrin activation was affected by the loss of NM II-A

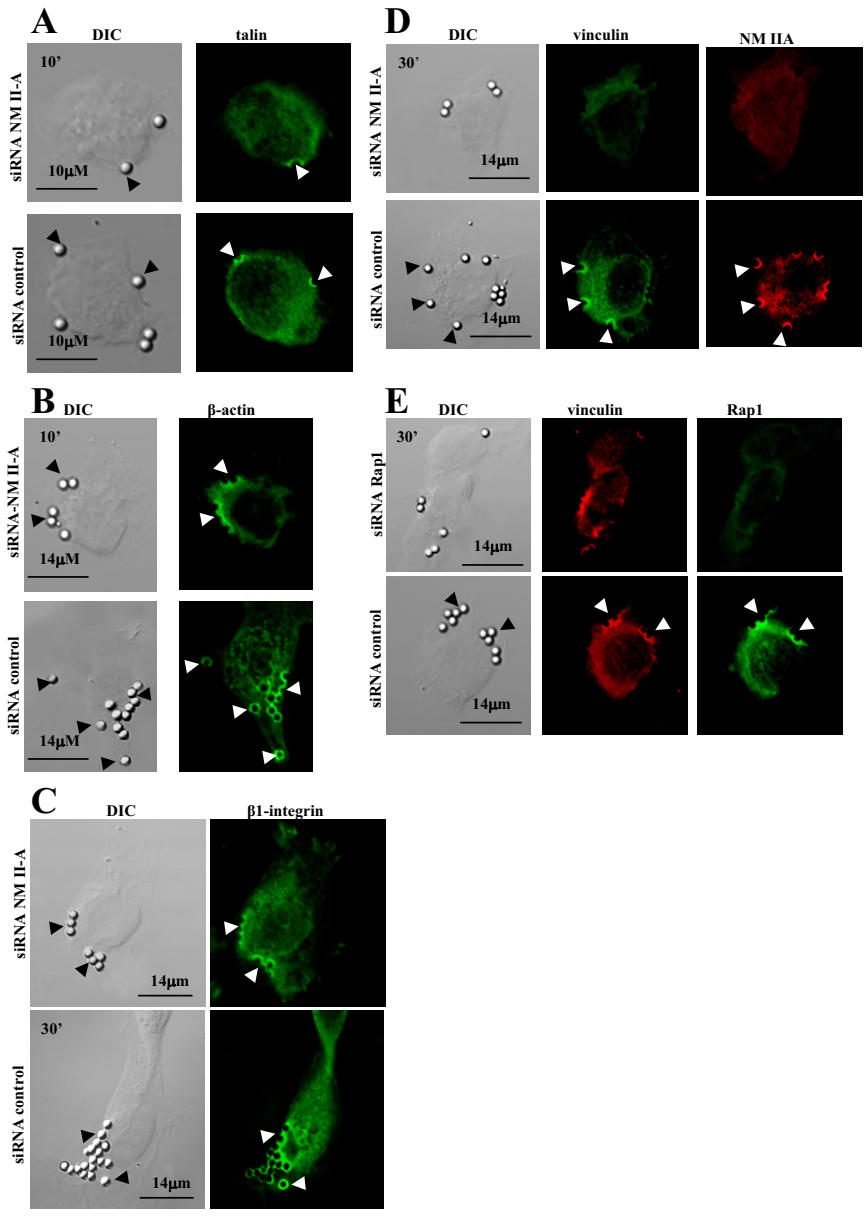

Figure 8. (A) Talin localizes to collagen beads at early times (10 min) independent of NM II-A knockdown (a–d). (B) β-actin accumulates around collagen beads at 10 min independent of NM II-A knockdown (a–d). (C) β1-integrin localizes to collagen beads in NM II-A knockdown and nontargeted siRNA-treated cells at 30 min after bead incubation. (D) Cells treated with NM II-A siRNA do not exhibit vinculin staining at collagen-bead sites, whereas nontargeted siRNA transfected cells show that vinculin associates with bound beads after 30 min. (E) Targeting of vinculin to collagen beads is not affected by knockdown of Rap1 by siRNA.

expression. There was reduced β1-integrin activation after collagen-bead binding in NM II-A null cells compared with NM II-B and WT cells at 30 min (Figure 7E).

Role of NM II-A at Collagen-Binding Sites

Because our data suggested that NM II-A regulates the activity and localization of Rap1 to collagen binding sites, we determined at what stage NM II-A is involved in the assembly of the collagen attachment complex. We examined molecules that assemble at the attachment complex with known kinetics for this system (Arora *et al.*, 2000). Talin and β-actin appear early, by 10 min after binding, whereas integrin and vinculin appear 30 min after binding. In NM II-A knockdown cells low NM II-A expression levels did not prevent localization of talin to collagen beads at 10 min after binding (Figure 8A). In cells with low levels of NM II-A, there were reduced numbers of bound collagen beads, but for those beads that did bind, there was normal staining for β-actin (Figure 8B) and β1-integrin (Figure 8C) at the bead-binding sites. In contrast vinculin was completely absent around bead sites at 30 min (Figure 8D). Notably, cells with Rap1 knockdown showed normal staining for vinculin at collagen-bead binding sites (Figure 8E). Further, treatment with blebbistatin did not affect assembly of actin around beads (Supplementary Figure S5) similar to findings with Fc-mediated phagocytosis (Tsai and Discher, 2008).

DISCUSSION

Collagen phagocytosis by connective tissue fibroblasts mediates extracellular matrix remodeling (Everts *et al.*, 1996). Unlike the phagocytosis exhibited by professional phagocytes such as macrophages (Caron and Hall, 1998), phagocytosis of fibrillar collagen by fibroblasts is much slower (Everts *et al.*, 1996), is largely dependent on integrins, and in particular, the $\alpha 2\beta 1$-integrin (Arora *et al.*, 2000), and is influenced by the actin-binding protein gelsolin (Arora *et al.*, 2005). Further, and as shown here, increased stiffness of

collagen has only a modest inhibitory effect on internalization, whereas the internalization of IgG-coated particles is greatly increased by substrate stiffness (Beningo and Wang, 2002). In this report we found that the small GTPase Rap1 enhances integrin-mediated adhesion (Bos *et al.*, 2003), but the molecular mechanisms recruiting Rap1 to integrins are not defined. We used collagen-bead binding to cultured fibroblasts (Arora *et al.*, 2003) as a model system for investigating the spatial localization, recruitment and activation of the signaling pathways that regulate $\alpha 2\beta 1$-integrin–dependent collagen phagocytosis. The main finding is that NM II-A is required for Rap1 targeting to $\beta 1$-integrin adhesion sites. The data indicate that collagen binding to $\alpha 2\beta 1$-integrin recruits NM II-A to the bead binding site, and promotes NM II-A phosphorylation. MLC phosphorylation enhances myosin II-A filament assembly and permits the binding of Rap1 to myosin II-A filaments. In a positive feedback loop, Rap1 enhances $\beta 1$-integrin activation and increased collagen adhesion to cells (Figure 9).

Rap1 Activation in Collagen Phagocytosis

We found that Rap1 was enriched around collagen beads after initial binding and that $\beta 1$-integrin ligation induced time-dependent activation of Rap1. Previous work has shown that Rap can activate collagen receptors, thereby increasing cell binding to matrix ligands mediated by $\beta 1$-integrins (Bos *et al.*, 2001), and can regulate the interaction of cells with the extracellular matrix (Reedquist *et al.*, 2000; Caron, 2003). Conversely our data also show that ligated $\beta 1$-integrins can activate Rap1 through a mechanism that is dependent on NM II-A. In this context it has been shown that signaling from $\beta 2$-integrin is required for Rap1 activation and for enhanced neutrophil adhesion (Jenei *et al.*, 2006).

We observed that the level of $\beta 1$-integrin activation markedly increased at collagen-bead binding sites for up to 30 min following collagen binding and declined thereafter. As expected the kinetics of Rap1 activation were contemporaneous with $\beta 1$-integrin activation. However, increased collagen-bead binding continued up to 120 min, even though Rap1 and $\beta 1$-integrin activities had subsided. These observations suggest that other collagen adhesion promoting molecules (e.g., discoidin domain receptors and endo180) likely play a role in the later stages of collagen phagocytosis. Further, Rap activation may be restricted to early phases of bead binding; after the initial steps of bead binding Rap1 is inactivated and the process continues independently of Rap. Conceivably, Rap is required for the initial bead binding state, but continuous Rap activity is not required to maintain it. What our data show is that in the early phases of collagen binding and phagocytosis, Rap1-integrin interactions are critical as shown by reduction of collagen binding and collagen film degradation after knockdown of Rap1 protein expression levels.

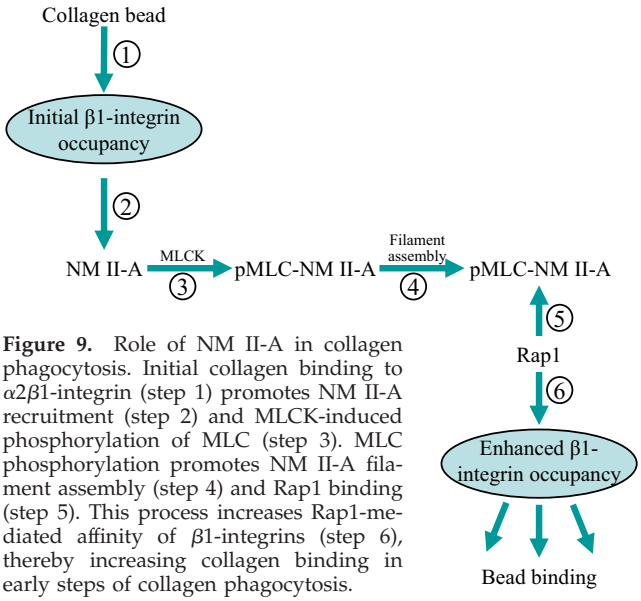

Figure 9. Role of NM II-A in collagen phagocytosis. Initial collagen binding to $\alpha 2\beta 1$-integrin (step 1) promotes NM II-A recruitment (step 2) and MLCK-induced phosphorylation of MLC (step 3). MLC phosphorylation promotes NM II-A filament assembly (step 4) and Rap1 binding (step 5). This process increases Rap1-mediated affinity of $\beta 1$-integrins (step 6), thereby increasing collagen binding in early steps of collagen phagocytosis.

Rap1 Interacts with NM II-A

$\beta 1$-integrin activation was enhanced at collagen binding sites, which also showed elevated Rap1 activity. Notably, we found that there was enhanced NM II-A association with Rap1 after collagen binding. These findings are consistent with the notion that NM II-A plays a crucial role in diverse functions such as cytokinesis, phagocytosis and cell polarity. In response to chemoattractant, Rap1 is activated and localizes to the leading edge of spreading *D. discoideum* cells (Jeon *et al.*, 2007). The proposed mechanism by which Rap1 controls cell spreading and attachment in *Dictyostelium* is partly through the phosphorylation-dependent regulation of NM II assembly. Our data also show that $\beta 1$-integrin affinity is dependent in part on phosphorylation of myosin light chains.

Our experiments with the myosin II ATPase inhibitor blebbistatin and with the Rho kinase inhibitor Y-27632 showed no detectable inhibition of collagen binding, whereas siRNA knockdown of MLCK or treatment with a MLCK inhibitor (ML-7) reduced collagen binding, interfered with collagen bead-induced Rap1/NM II-A interactions and blocked Rap1 activation. In vitro studies have shown that NM II filament assembly and motor activity are controlled by MLC phosphorylation on Thr18/Ser19 (Ikebe and Hartshorne, 1985). Taken together these experiments suggest that it is not activation of the NM II-A motor (as would be suggested by inhibition with blebbistatin) but rather filament assembly that allows NM II-A to function as a Rap1 adaptor at the sites of the collagen-integrin attachment, which in turn is required for collagen binding and internalization. In this context Triton-permeabilization experiments showed that NM II-A filaments colocalized with filamentous actin at collagen bead sites. Collectively our data suggest that NM II-A filament assembly is important for Rap1 binding and as a result, $\beta 1$-integrin activation and enhanced collagen binding.

Rap1 knockdown cells showed normal localization of NM II-A to collagen beads, indicating that NM II-A is targeted to collagen adhesion sites independent of Rap1, and may function as an adaptor protein that links Rap1 and integrins. Although Rap1 is activated by a large number of stimuli and second messengers, which then activate guanine nucleotide exchange factors, the downstream effectors of Rap1 are less well defined (Bos, 2005).

Regulation of Rap1 by NM II-A

The use of NM II-A and II-B null ES cells to determine the specificity of NM II-A–mediated regulation of Rap1 during collagen phagocytosis support siRNA studies showing that NM II-A is required for collagen-induced Rap1 activation. Our data show that collagen binding enhanced the association of $\beta 1$-integrins with NM II-A, whereas the absence of NM II-A, but not NM II-B prevented collagen-induced Rap1 activation. Despite the high level of amino acid conservation between the nonmuscle myosin II isoforms, they exhibit

difference in motor activity and localization (Kovacs *et al.*, 2003; Wang *et al.*, 2003). Studies have suggested that NM II-A and II-B assembly/disassembly are regulated separately. Notably, NM II-A heavy-chain phosphorylation regulates motility and lamellipod extension (Dulyaninova *et al.*, 2005), whereas cyclic assembly of NM II-B filaments has a role in generating the power for three-dimensional collagen fiber movement (Meshel *et al.*, 2005).

Although NM II-A may regulate Rap1 localization to collagen-binding sites, it is not involved in regulating some of the proteins that form the collagen attachment complex including talin, actin, and β1-integrin, which appear at the collagen attachment complex independent of NM II-A. In this context initial activation of integrins by attachment to matrix proteins promotes the binding of β1-integrin cytoplasmic tails to talin (Tadokoro *et al.*, 2003). However, we observed that reduced levels of NM II-A after siRNA knockdown prevented targeting of vinculin to collagen bead sites, which is consistent with earlier data showing lack of vinculin at adhesion sites in NM II-A null ES cells but not NM II-B ES cells (Even-Ram *et al.*, 2007). These observations suggest that NM II-A is critical for vinculin recruitment and for subsequent steps of β1-integrin activation.

In conclusion we show that NM II-A associates with Rap1 and is important for collagen-dependent targeting and activation. The targeting of Rap1 to collagen binding sites in a NM II-A–dependent manner may provide a system by which integrin activation and Rap1 activation amplify one another locally to enhance collagen phagocytosis.

ACKNOWLEDGMENTS

We thank Tarek El Sayegh for reading the manuscript and for helpful suggestions, Cheung Lo for cell culture, and Wilson Lee for flow cytometry. This work was supported by Canadian Institutes of Health Research operating (416228), group (450695), and major equipment grants (C.A.M.).

REFERENCES

Arora, P. D., Chan, M. W., Anderson, R. A., Janmey, P. A., and McCulloch, C. A. (2005). Separate functions of gelsolin mediate sequential steps of collagen phagocytosis. Mol. Biol. Cell *16*, 5175–5190.

Arora, P. D., Fan, L., Sodek, J., Kapus, A., and McCulloch, C. A. (2003). Differential binding to dorsal and ventral cell surfaces of fibroblasts: effect on collagen phagocytosis. Exp. Cell Res. *286*, 366–380.

Arora, P. D., Manolson, M. F., Downey, G. P., Sodek, J., and McCulloch, C. A. (2000). A novel model system for characterization of phagosomal maturation, acidification, and intracellular collagen degradation in fibroblasts. J. Biol. Chem. *275*, 35432–35441.

Arora, P. D., Narani, N., and McCulloch, C. A. (1999). The compliance of collagen gels regulates transforming growth factor-beta induction of alpha-smooth muscle actin in fibroblasts. Am J. Pathol. *154*, 871–882.

Arthur, W. T., Quilliam, L. A., and Cooper, J. A. (2004). Rap1 promotes cell spreading by localizing Rac guanine nucleotide exchange factors. J. Cell Biol. *167*, 111–122.

Beningo, K. A., and Wang, Y. L. (2002). Fc-receptor-mediated phagocytosis is regulated by mechanical properties of the target. J. Cell Sci. *115*, 849–856.

Bivona, T. G., Wiener, H. H., Ahearn, I. M., Silletti, J., Chiu, V. K., and Philips, M. R. (2004). Rap1 up-regulation and activation on plasma membrane regulates T cell adhesion. J. Cell Biol. *164*, 461–470.

Bolte, S., and Cordelieres, F. P. (2006). A guided tour into subcellular colocalization analysis in light microscopy. J. Micros. *224*, 213–232.

Bos, J. L. (2005). Linking Rap to cell adhesion. Curr. Opin. Cell Biol. *17*, 123–128.

Bos, J. L., de Bruyn, K., Enserink, J., Kuiperij, B., Rangarajan, S., Rehmann, H., Riedl, J., de Rooij, J., van Mansfeld, F., and Zwartkruis, F. (2003). The role of Rap1 in integrin-mediated cell adhesion. Biochem. Soc. Trans. *31*, 83–86.

Bos, J. L., de Rooij, J., and Reedquist, K. A. (2001). Rap1 signalling: adhering to new models. Nat. Rev. Mol. Cell Biol. *2*, 369–377.

Caron, E. (2003). Cellular functions of the Rap1 GTP-binding protein: a pattern emerges. J. Cell Sci. *116*, 435–440.

Caron, E., and Hall, A. (1998). Identification of two distinct mechanisms of phagocytosis controlled by different Rho GTPases. Science *282*, 1717–1721.

Caron, E., Self, A. J., and Hall, A. (2000). The GTPase Rap1 controls functional activation of macrophage integrin alphaMbeta2 by LPS and other inflammatory mediators. Curr. Biol. *10*, 974–978.

Castro, A. F., Rebhun, J. F., and Quilliam, L. A. (2005). Measuring Ras-family GTP levels in vivo–running hot and cold. Methods *37*, 190–196.

Cheney, R. E., and Mooseker, M. S. (1992). Unconventional myosins. Curr. Opin. Cell Biol. *4*, 27–35.

Chrzanowska-Wodnicka, M., and Burridge, K. (1996). Rho-stimulated contractility drives the formation of stress fibers and focal adhesions. J. Cell Biol. *133*, 1403–1415.

Conti, M. A., Even-Ram, S., Liu, C., Yamada, K. M., and Adelstein, R. S. (2004). Defects in cell adhesion and the visceral endoderm following ablation of nonmuscle myosin heavy chain II-A in mice. J. Biol. Chem. *279*, 41263–41266.

Cougoule, C., Hoshino, S., Dart, A., Lim, J., and Caron, E. (2006). Dissociation of recruitment and activation of the small G-protein Rac during Fcgamma receptor-mediated phagocytosis. J. Biol. Chem. *281*, 8756–8764.

Cougoule, C., Wiedemann, A., Lim, J., and Caron, E. (2004). Phagocytosis, an alternative model system for the study of cell adhesion. Semin. Cell Dev. Biol. *15*, 679–689.

Curino, A. C., Engelholm, L. H., Yamada, S. S., Holmbeck, K., Lund, L. R., Molinolo, A. A., Behrendt, N., Nielsen, B. S., and Bugge, T. H. (2005). Intracellular collagen degradation mediated by uPARAP/Endo180 is a major pathway of extracellular matrix turnover during malignancy. J. Cell Biol. *169*, 977–985.

de Bruyn, K. M., Rangarajan, S., Reedquist, K. A., Figdor, C. G., and Bos, J. L. (2002). The small GTPase Rap1 is required for Mn(2+)- and antibody-induced LFA-1- and VLA-4-mediated cell adhesion. J. Biol. Chem. *277*, 29468–29476.

Del Pozo, M. A., Kiosses, W. B., Alderson, N. B., Meller, N., Hahn, K. M., and Schwartz, M. A. (2002). Integrins regulate GTP-Rac localized effector interactions through dissociation of Rho-GDI. Nat. Cell Biol *4*, 232–239.

Dulyaninova, N. G., Malashkevich, V. N., Almo, S. C., and Bresnick, A. R. (2005). Regulation of myosin-IIA assembly and Mts1 binding by heavy chain phosphorylation. Biochemistry *44*, 6867–6876.

Even-Ram, S., Doyle, A. D., Conti, M. A., Matsumoto, K., Adelstein, R. S., and Yamada, K. M. (2007). Myosin IIA regulates cell motility and actomyosin-microtubule crosstalk. Nat. Cell Biol. *9*, 299–309.

Everts, V., van der Zee, E., Creemers, L., and Beertsen, W. (1996). Phagocytosis and intracellular digestion of collagen, its role in turnover and remodelling. Histochem. J. *28*, 229–245.

Garrett, S. C., Hodgson, L., Rybin, A., Toutchkine, A., Hahn, K. M., Lawrence, D. S., and Bresnick, A. R. (2008). A biosensor of S100A4 metastasis factor activation: inhibitor screening and cellular activation dynamics. Biochemistry *47*, 986–996.

Grinnell, F. (1980). Fibroblast receptor for cell-substratum adhesion: studies on the interaction of baby hamster kidney cells with latex beads coated by cold insoluble globulin (plasma fibronectin). J. Cell Biol. *86*, 104–112.

Hall, A. B., Gakidis, M. A., Glogauer, M., Wilsbacher, J. L., Gao, S., Swat, W., and Brugge, J. S. (2006). Requirements for Vav guanine nucleotide exchange factors and Rho GTPases in FcgammaR- and complement-mediated phagocytosis. Immunity *24*, 305–316.

Han, J. *et al.* (2006). Reconstructing and deconstructing agonist-induced activation of integrin alphaIIbbeta3. Curr. Biol. *16*, 1796–1806.

Hu, A., Wang, F., and Sellers, J. R. (2002). Mutations in human nonmuscle myosin IIA found in patients with May-Hegglin anomaly and Fechtner syndrome result in impaired enzymatic function. J. Biol. Chem. *277*, 46512–46517.

Hughes, P. E., and Pfaff, M. (1998). Integrin affinity modulation. Trends Cell Biol. *8*, 359–364.

Ikebe, M., and Hartshorne, D. J. (1985). Phosphorylation of smooth muscle myosin at two distinct sites by myosin light chain kinase. J. Biol. Chem. *260*, 10027–10031.

Jenei, V., Deevi, R. K., Adams, C. A., Axelsson, L., Hirst, D. G., Andersson, T., and Dib, K. (2006). Nitric oxide produced in response to engagement of beta2 integrins on human neutrophils activates the monomeric GTPases Rap1 and Rap2 and promotes adhesion. J. Biol. Chem. *281*, 35008–35020.

Jeon, T. J., Lee, D. J., Merlot, S., Weeks, G., and Firtel, R. A. (2007). Rap1 controls cell adhesion and cell motility through the regulation of myosin II. J. Cell Biol. *176*, 1021–1033.

Jeong, H. W., Li, Z., Brown, M. D., and Sacks, D. B. (2007). IQGAP1 Binds Rap1 and Modulates Its Activity. J. Biol. Chem. *282*, 20752–20762.

Kang, R., Kae, H., Ip, H., Spiegelman, G. B., and Weeks, G. (2002). Evidence for a role for the *Dictyostelium* Rap1 in cell viability and the response to osmotic stress. J. Cell Sci. *115*, 3675–3682.

Kinashi, T., and Katagiri, K. (2005). Regulation of immune cell adhesion and migration by regulator of adhesion and cell polarization enriched in lymphoid tissues. Immunology *116*, 164–171.

Kovacs, M., Wang, F., Hu, A., Zhang, Y., and Sellers, J. R. (2003). Functional divergence of human cytoplasmic myosin II: kinetic characterization of the non-muscle IIA isoform. J. Biol. Chem. *278*, 38132–38140.

Lafuente, E. M., van Puijenbroek, A. A., Krause, M., Carman, C. V., Freeman, G. J., Berezovskaya, A., Constantine, E., Springer, T. A., Gertler, F. B., and Boussiotis, V. A. (2004). RIAM, an Ena/VASP and Profilin ligand, interacts with Rap1-GTP and mediates Rap1-induced adhesion. Dev. Cell *7*, 585–595.

Lee, H., Overall, C. M., McCulloch, C. A., and Sodek, J. (2006). A critical role for the membrane-type 1 matrix metalloproteinase in collagen phagocytosis. Mol. Biol. Cell *17*, 4812–4826.

Li, Z. H., Spektor, A., Varlamova, O., and Bresnick, A. R. (2003). Mts1 regulates the assembly of nonmuscle myosin-IIA. Biochemistry *42*, 14258–14266.

McAbee, D. D., and Grinnell, F. (1983). Fibronectin-mediated binding and phagocytosis of polystyrene latex beads by baby hamster kidney cells. J. Cell Biol. *97*, 1515–1523.

McCulloch, C. A. (2004). Drug-induced fibrosis: interference with the intracellular collagen degradation pathway. Curr. Opin. Drug Discov. Devel. *7*, 720–724.

Meshel, A. S., Wei, Q., Adelstein, R. S., and Sheetz, M. P. (2005). Basic mechanism of three-dimensional collagen fibre transport by fibroblasts. Nat. Cell Biol. *7*, 157–164.

Mould, A. P., and Humphries, M. J. (2004). Regulation of integrin function through conformational complexity: not simply a knee-jerk reaction? Curr. Opin. Cell Biol. *16*, 544–551.

Olazabal, I. M., Caron, E., May, R. C., Schilling, K., Knecht, D. A., and Machesky, L. M. (2002). Rho-kinase and myosin-II control phagocytic cup formation during CR, but not FcgammaR, phagocytosis. Curr. Biol. *12*, 1413–1418.

Pappin, D. J., Hojrup, P., and Bleasby, A. J. (1993). Rapid identification of proteins by peptide-mass fingerprinting. Curr. Biol. *3*, 327–332.

Pollard, T. D., Doberstein, S. K., and Zot, H. G. (1991). Myosin-I. Annu. Rev. Physiol. *53*, 653–681.

Price, L. S., Leng, J., Schwartz, M. A., and Bokoch, G. M. (1998). Activation of Rac and Cdc42 by integrins mediates cell spreading. Mol. Biol. Cell *9*, 1863–1871.

Rebstein, P. J., Weeks, G., and Spiegelman, G. B. (1993). Altered morphology of vegetative amoebae induced by increased expression of the *Dictyostelium discoideum* ras-related gene rap1. Dev. Genet. *14*, 347–355.

Reedquist, K. A., Ross, E., Koop, E. A., Wolthuis, R. M., Zwartkruis, F. J., van Kooyk, Y., Salmon, M., Buckley, C. D., and Bos, J. L. (2000). The small GTPase, Rap1, mediates CD31-induced integrin adhesion. J. Cell Biol. *148*, 1151–1158.

Retta, S. F., Balzac, F., and Avolio, M. (2006). Rap1, a turnabout for the crosstalk between cadherins and integrins. Eur. J. Cell Biol. *85*, 283–293.

Seastone, D. J., Zhang, L., Buczynski, G., Rebstein, P., Weeks, G., Spiegelman, G., and Cardelli, J. (1999). The small Mr Ras-like GTPase Rap1 and the phospholipase C pathway act to regulate phagocytosis in *Dictyostelium discoideum*. Mol. Biol. Cell *10*, 393–406.

Sellers, J. R. (2000). Myosins: a diverse superfamily. Biochim. Biophys. Acta *1496*, 3–22.

Small, J. V. (1981). Organization of actin in the leading edge of cultured cells: influence of osmium tetroxide and dehydration on the ultrastructure of actin meshworks. J. Cell Biol. *91*, 695–705.

Tadokoro, S., Shattil, S. J., Eto, K., Tai, V., Liddington, R. C., de Pereda, J. M., Ginsberg, M. H., and Calderwood, D. A. (2003). Talin binding to integrin beta tails: a final common step in integrin activation. Science *302*, 103–106.

Tsai, R. K., Discher, D. E. (2008). Inhibition of "self" engulfment through deactivation of myosin-II at the phagocytic synapse between human cells. J. Cell Biol. *180*, 989–1003.

Vicente-Manzanares, M., Zareno, J., Whitmore, L., Choi, C. K., and Horwitz, A. F. (2007). Regulation of protrusion, adhesion dynamics, and polarity by myosins IIA and IIB in migrating cells. J. Cell Biol. *176*, 573–580.

Wang, F., Kovacs, M., Hu, A., Limouze, J., Harvey, E. V., and Sellers, J. R. (2003). Kinetic mechanism of non-muscle myosin IIB: functional adaptations for tension generation and maintenance. J. Biol. Chem. *278*, 27439–27448.

Watanabe, T., Hosoya, H., and Yonemura, S. (2007). Regulation of myosin II dynamics by phosphorylation and dephosphorylation of its light chain in epithelial cells. Mol. Biol. Cell *18*, 605–616.